Supporting Information

Photocatalytic Transfer Hydrogenation of Nitriles to Primary Amines over a Pd Nanocube-Modified Poly(heptazine imide) Catalyst

Chong Wang [a, b], Wenwen Tian [a], Yichun Lu [c], Hongyu Chen [a], Zhu Yin [a], Jingru Zhuang [b], Huali Zhang [a], Liuyong Chen [d], Oleksandr Savateev [b]*, Jiajia Cheng [a]**

a. State Key Laboratory of Chemistry for NBC Hazards Protection and State Key Laboratory of Photocatalysis on Energy and Environment, College of Chemistry, Fuzhou University, Fuzhou 350116, China. Email: jjcheng@fzu.edu.cn

b. Department of Chemistry, The Chinese University of Hong Kong, Shatin, Hong Kong SAR 999077, China. Email: oleksandrsavatieiev@cuhk.edu.hk

c. State Key Laboratory of Marine Environmental Health, City University of Hong Kong, Kowloon Tong, Hong Kong SAR 999077, China. Email: yichun.lu@cityu.edu.hk

d. School of Chemistry and Chemical Engineering, Lingnan Normal University, Zhanjiang 524048, China.

S1 Experimental section

S1.1 Synthesis of samples

S1.1.1 Synthesis of Pd nanotubes. Under stirring conditions, 0.5 mL of a 10 mmol·L^{-1} dihydrogen tetrachloropalladate (H_2PdCl_4) solution was added dropwise into 10 mL of a 12.5 mmol·L^{-1} cetyltrimethylammonium bromide (CTAB) solution. Subsequently, the mixture was heated to 95 °C and maintained at this temperature for 5 minutes. Then, 80 μL of a freshly prepared 100 mmol·L^{-1} ascorbic acid solution was added, and the reaction was allowed to proceed for an additional 10 minutes.

S1.1.2 Synthesis of Pd nanorods. Under stirring conditions, 125 μL of a 10 mmol·L^{-1} dihydrogen tetrachloropalladate (H_2PdCl_4) solution was added to 5 mL of a 50 mmol·L^{-1} CTAB solution, and the mixture was maintained at 40 °C. Then, 400 μL of the pre-synthesized Pd nanocube solution was added, followed by the introduction of 25 μL of a freshly prepared 100 mmol·L^{-1} ascorbic acid solution, with thorough mixing. The resulting solution was placed in a water bath at 40 °C, and the reaction was terminated after 24 hours.

S1.1.3 Synthesis of poly(heptazine imide) (PHI). Melamine (8 g) was placed in a covered crucible and warmed to 550 ℃ for 4 hours at a rate of 2.2 ℃·min^{-1} in a muffle furnace. The yellow solid was denoted as bulk carbon nitride. 3.7 g of KCl and 2.7 g of LiCl were ground with 600 mg of bulk carbon nitride for 10 minutes. Then, the mixture was put into a corundum boat with a cover and heated to 550 ℃ for 4 hours under a N_2 atmosphere (200 mL·min^{-1}) in a tube furnace. The heating rate was 2.2 ℃·min^{-1}. After natural cooling, the mixture was poured into boiling distilled water and collected by filtration. After drying at 60 ℃ under vacuum for 10 hours, the powder samples were obtained, denoted as PHI.

S1.1.4 Synthesis of Pd nanocube-modified PHI (C-Pd-PHI). 100 mg of PHI was dispersed in 20 mL of water. A solution of Pd nanocubes (3 mg of Pd) was then added. The mixed suspension was sonicated for 30 minutes and stirred overnight. The sample was washed with deionized water and ethanol several times and dried at 60 ℃ under vacuum for 10 hours. The solid sample was denoted as C-Pd-PHI (C refers to cube).

S1.1.5 Synthesis of Pd nanorod-modified PHI (R-Pd-PHI). 100 mg of PHI was dispersed in 20 mL of water. A solution of Pd nanorods (3 mg of Pd) was then added. The mixed suspension was sonicated for 30 minutes and stirred overnight. The sample was washed with deionized water and ethanol several times and dried at 60 ℃ under vacuum for 10 hours. The solid sample was denoted as R-Pd-PHI (R refers to rod).

S1.1.6 Synthesis of amorphous Pd nanoparticles-modified PHI (A-Pd-PHI). 100 mg of PHI was dispersed in 40 mL of a 25% methanol/water solution under magnetic stirring. Subsequently, a hydrochloric acid solution containing 3 mg of Pd was added to the suspension under a nitrogen atmosphere. The mixture was then irradiated with a xenon lamp for 3 hours. The mixture was washed with deionized water and ethanol and dried at 60 ℃ under vacuum for 10 hours. The solid sample was denoted as A-Pd-PHI (A refers to amorphous).

S1.1.7 Synthesis of 2-(3-chloro-5-(trifluoromethyl)pyridin-2-yl)acetonitrile.

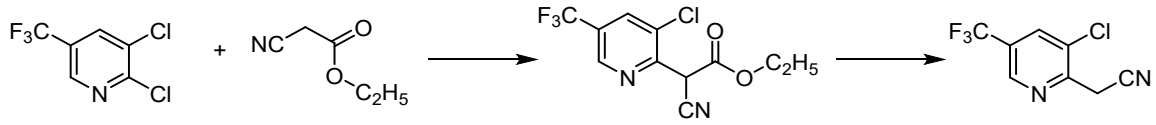

A mixture of 2,3-dichloro-5-(trifluoromethyl)pyridine (DCTF, 2.715 g, 12.5 mmol, 1.0 equiv., 99.5%), N-methylpyrrolidone (NMP, 10 mL), and solid potassium hydroxide (1.24 g, 22.1 mmol, 1.7 equiv., 99%) was added into a 100 mL three-necked flask. The reaction mixture was stirred and heated to 70–80 ℃. Ethyl cyanoacetate (1.715 g, 15.0 mmol, 1.2 equiv., 99%) was added dropwise over approximately 2 minutes, during which an exotherm was observed. The temperature was maintained at 70–80 ℃, and the reaction was stirred for 6 hours at this temperature. Reaction completion was monitored by tin layer chromatography (TLC), indicating full consumption of the starting material. Concentrated hydrochloric acid (3.8 g, 37.5 mmol, 3.0 equiv., 36% w/w) was then added dropwise. The resulting mixture was heated under reflux and stirred overnight. TLC analysis confirmed the complete consumption of the intermediate, affording a brownish-yellow suspension. After cooling to ambient temperature, water (20 mL) was added, and the mixture was

stirred to dissolve soluble components. The aqueous phase was extracted with ethyl acetate (20 mL). The organic layer was back-extracted with water to remove excess NMP. The combined organic phase was concentrated under reduced pressure to give a crude mixture containing 2-(3-chloro-5-(trifluoromethyl)pyridin-2-yl)acetonitrile. The product was purified by column chromatography to afford 2.0 g of the target compound as a brown liquid in 72% yield.

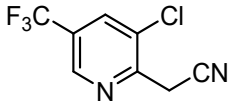

2-(3-chloro-5-(trifluoromethyl)pyridin-2-yl)acetonitrile: ^{1}H NMR (600 MHz, Chloroform-*d*) NMR δ 8.79 (d, J = 1.8 Hz, 1H), 7.98 (d, J = 1.9 Hz, 1H), 4.13 (s, 2H). ^{19}F NMR (600 MHz, Chloroform-d) δ -62.29 (s，3F)

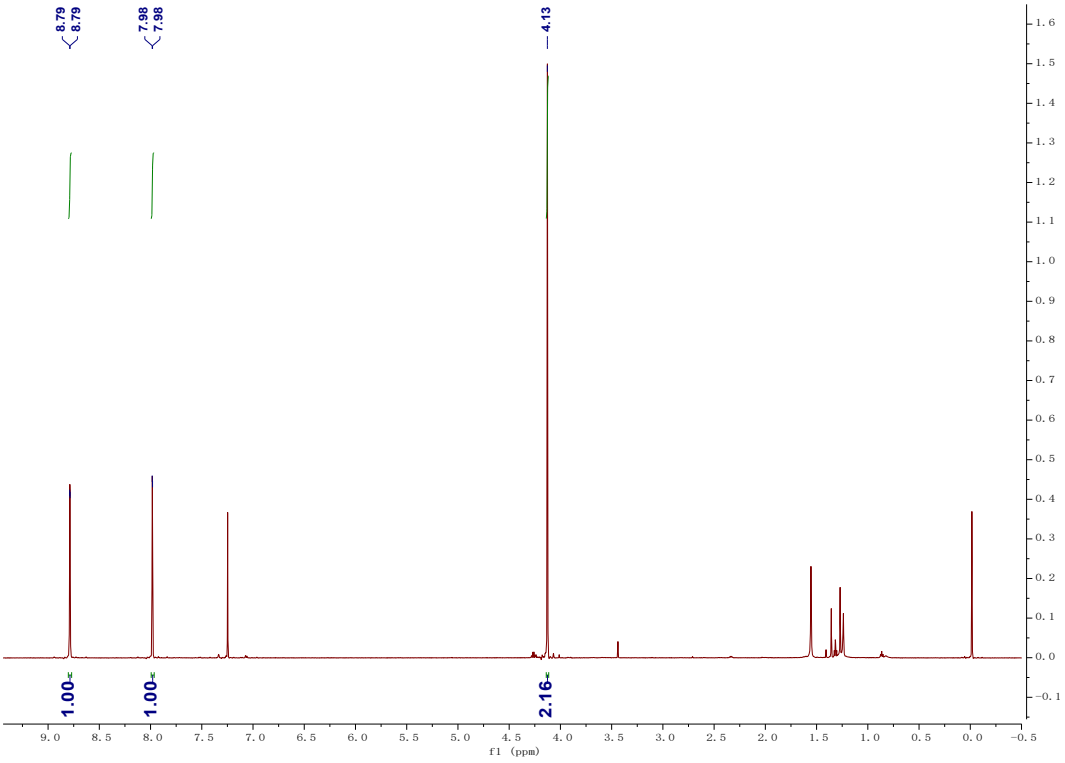

The ^{1}H NMR spectrum of 2-(3-chloro-5-(trifluoromethyl)pyridin-2-yl)acetonitrile.

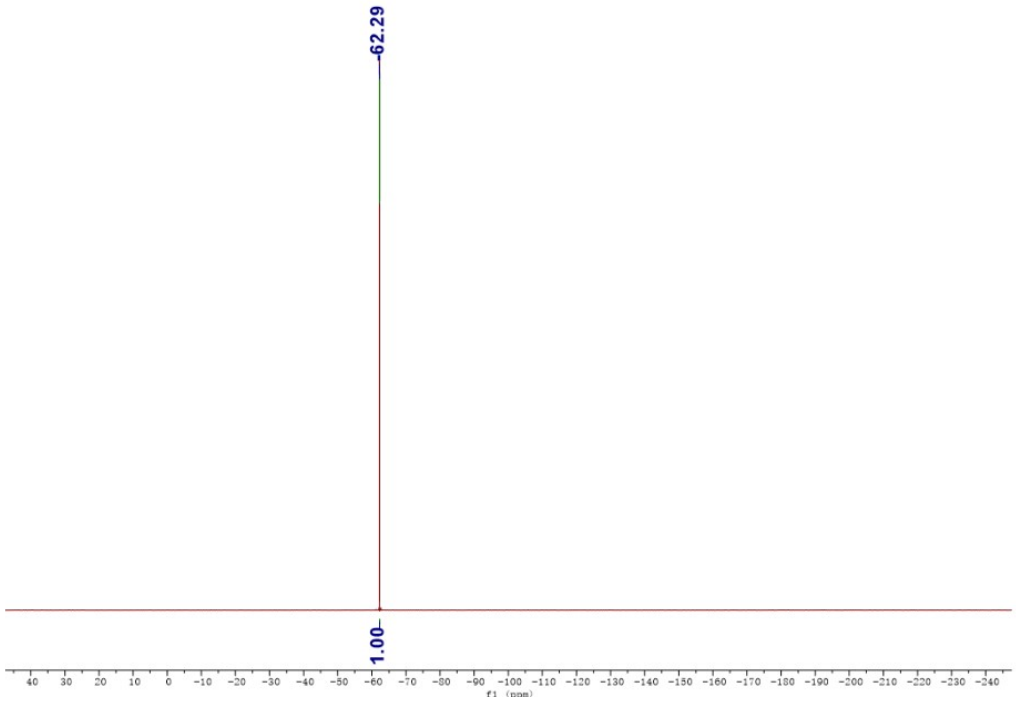

The ^{19}F NMR spectrum of 2-(3-chloro-5-(trifluoromethyl)pyridin-2-yl)acetonitrile.

S1.2 Characterizations

The Fourier transform infrared (FTIR) spectra of the samples were acquired using a Nicolet iS-50 instrument (Thermo) at the scan range of 400–4000 cm^{-1}. X-ray photoelectron spectroscopy (XPS) data were acquired using a Thermo ESCALAB 250Xi instrument equipped with a monochromatized Al Kα (200 W) as the excitation source. The binding energy was referenced to the adventitious C 1s peak at 284.80 eV. UV–vis diffuse reflectance spectra (DRS) were recorded using PerkinElmer UV/Vis/NIR Spectrometer Lambda 950 and Agilent Cary Series UV–vis Spectrometer in a diffuse reflectance mode. The ultraviolet photoelectron spectroscopy (UPS) data were obtained on a Thermo ESCALAB 250Xi equipped with a He-I source (21.22 eV) and calibrated by Au. The morphology and microstructure of samples were characterized by SEM (SU8010) and TEM (Taios F200S). X-ray diffraction (XRD) patterns were acquired using a Rigaku Miniflex powder diffractometer (Cu Kα radiation, 40 kV and 15 mA) with a scan 2θ range of 5–80 degrees. Electron paramagnetic resonance (EPR) measurements were conducted on a Bruker model A300 spectrometer. The Micromeritics 2460 adsorption analyzer was

used to carry out N_2 (77 K) adsorption-desorption measurement and BET analysis. Room-temperature photoluminescence (PL) spectra were recorded on a Horiba Fluorolog-3 spectrophotometer using an Xe lamp (325 nm) as the excitation light source. Electron paramagnetic resonance (EPR) signals were quantitatively collected on a Bruker model A300 electron paramagnetic resonance at room temperature, equipped with a 50 W 420 nm LED lamp. Metal contents were measured by an inductively coupled plasma-optical emission spectrometer (ICP-OES) (PerkinElmer, Avio 200). The Zeta potential of the materials was tested using Malvern's ZS90 nanoparticle size and Zeta potential analyzer. The electrochemical impedance, Mott-Schottky, and photocurrent response of the catalysts were measured on the electrochemical workstation (Bio-Logic, VSP-300). Hydrogen temperature programmed desorption (H_2-TPD) measurements were carried out on a Micromeritics AutoChem II 2920 Chemisorption Analyzer. Before testing, the catalyst sample was heated to 150 ℃ (30 min) in an argon atmosphere to remove surface impurities. The test temperature ranges from 50 to 700 ℃, with a heating rate of 10 ℃ per minute. HPLC analysis was carried out using an Agilent G7129A instrument fitted with a C18 reversed-phase column. The chromatographic conditions were established as: mobile phase comprising water (with 0.01% v/v trifluoroacetic acid) and acetonitrile (50:50, v/v); column oven temperature maintained at 35 ℃; and detection wavelength of 280 nm.

S1.3 Photo-electrochemical measurements

Electrochemical measurements were conducted in a standard three-electrode system, using a Pt plate as the counter electrode and a silver chloride electrode (Ag/AgCl) as the reference electrode. The working electrode was prepared on a F-doped SnO_2-coated glass (FTO glass), which was cleaned by sonication in ethanol for 30 min and dried at 25 ℃. The working electrodes were prepared by dip-coating as follows: 5 mg of the sample was dispersed in 2 mL of N,N-dimethylformamide (DMF) by sonication to give a slurry mixture. 10 μL of the slurry was spread onto the pretreated FTO glass. The electrolyte was a 0.2 M Na_2SO_4 aqueous solution without an additive (pH = 7). Electrochemical

impedance spectroscopy and the data for Mott-Schottky analysis were acquired without any irradiation. Photocurrent response experiments were conducted by alternating the periods of the electrode irradiation with light, followed by the current measurements in the dark.

S1.4 Photocatalytic transfer hydrogenation experiment of aliphatic nitriles

A 10 mL Schlenk tube was charged sequentially with 0.08 mmol of 2-(3-chloro-5-(trifluoromethyl)pyridin-2-yl)acetonitrile, 10 mg of photocatalyst, and a magnetic stir bar. Then, 3 mL of a mixed solvent composed of 0.1 M aqueous HCl and isopropanol (1:2, v/v) was added. The reaction was conducted under irradiation using a 420 nm LED light source for 12 hours at 25 ℃. After completion, 100 μL of the reaction mixture was diluted with acetonitrile to 1 mL and analyzed by high-performance liquid chromatography (HPLC) using the normalization method for quantification.

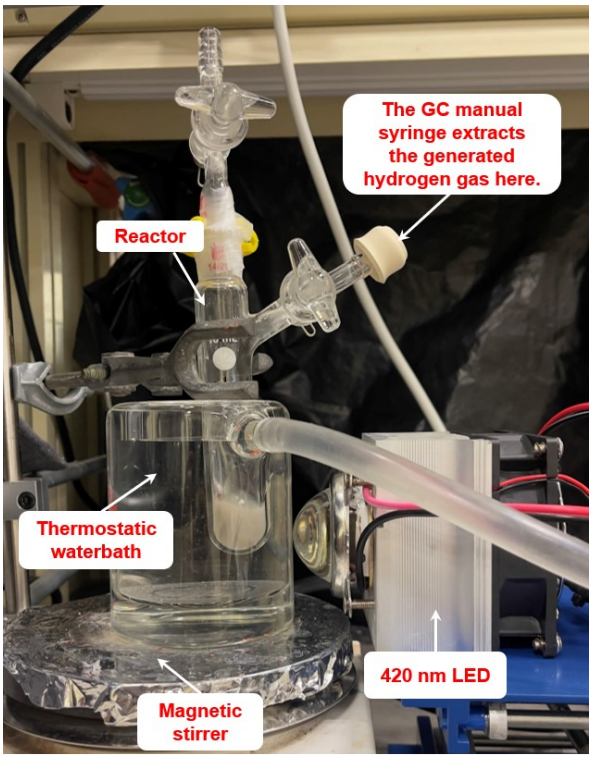

The photograph of photocatalytic reaction set-up.

S1.5 Theoretical calculation

Density functional theory (DFT) calculations were used for bond order calculations,

using the hybrid exchange-correlation functional B3LYP/6-311g. The bond order calculation was carried out using Gaussian 16[S1], and the post-processing was performed with the Multiwfn software[S2].

S2 Additional figures and tables

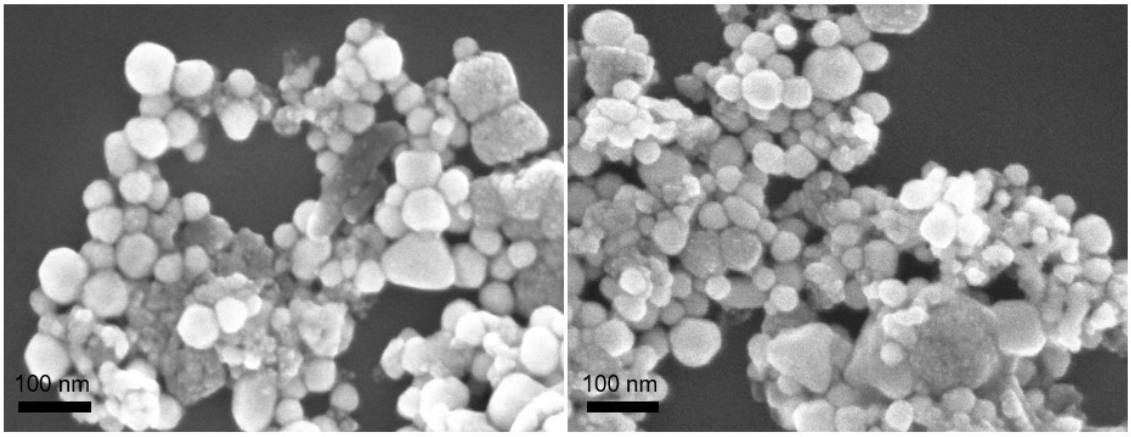

Figure S1. The SEM images of the Pd nanoparticles synthesized without using cetyltrimethylammonium bromide.

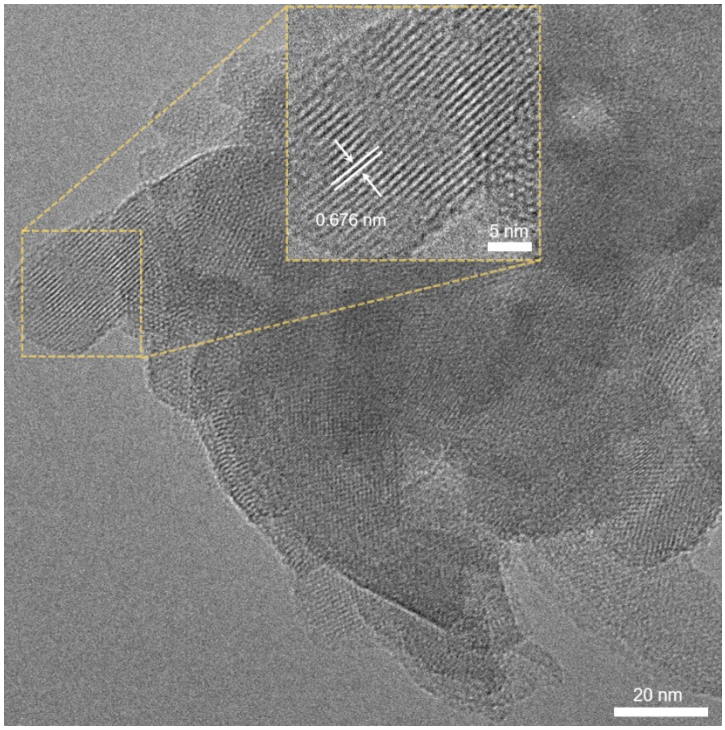

Figure S2. The TEM image of PHI.

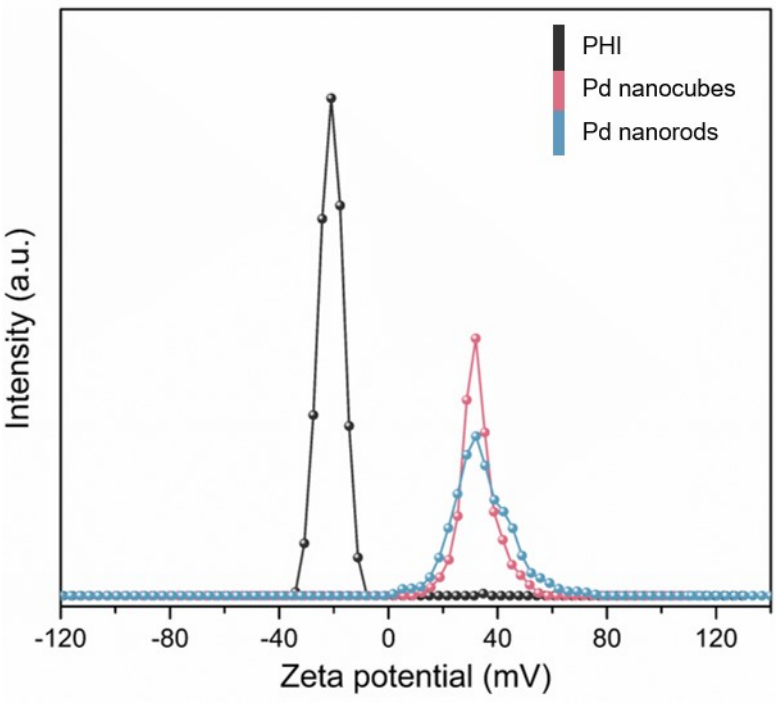

Figure S3. Zeta potential of the samples.

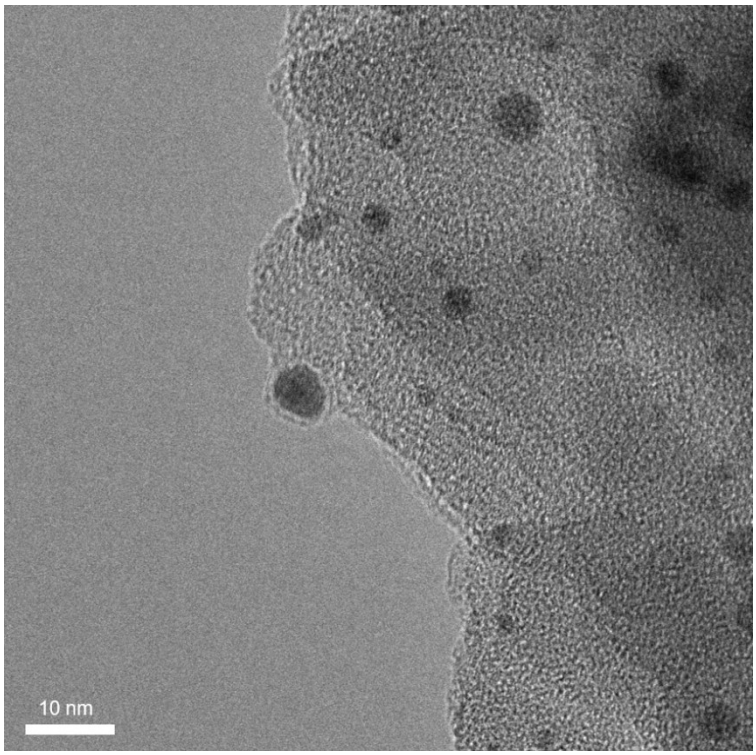

Figure S4. The TEM image of A-Pd-PHI.

Table S1. ICP-OES results of the samples.

Entry	Sample	Theoretical Pd dosage (wt%)	Actual Pd content (wt%)
1	PHI	0	0
2	A-Pd-PHI	3.0	1.5
3	C-Pd-PHI	3.0	2.2
4	R-Pd-PHI	3.0	2.4

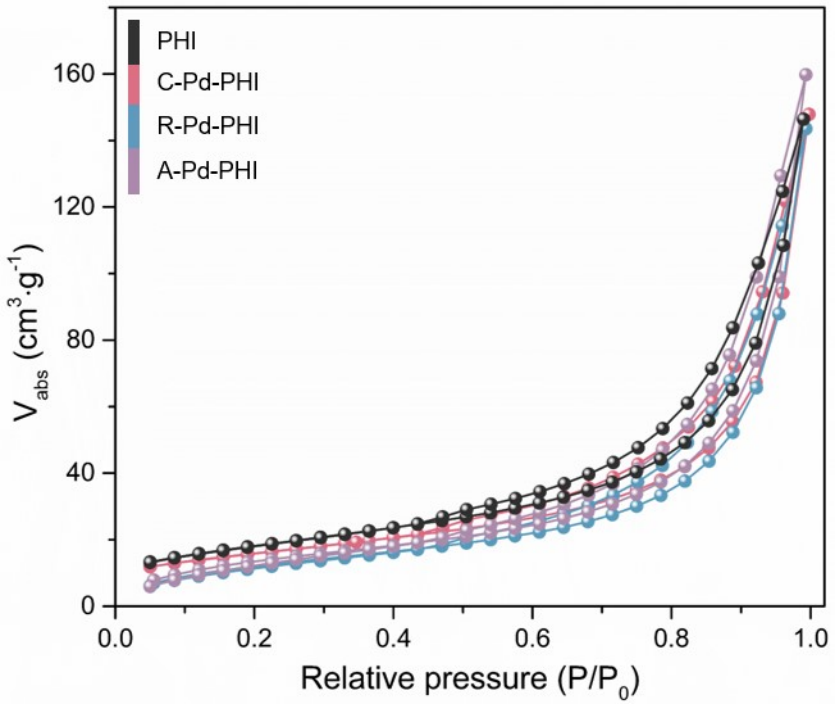

Figure S5. The N_2 adsorption-desorption isotherms of the samples.

Table S2. The porosity information of samples.

Entry	Sample	SA[a] [m^2 g^{-1}]	PV[b] [cm^3 g^{-1}]	PD[c] [nm]
1	PHI	65	0.19	12
2	C-Pd-PHI	47	0.22	14
3	R-Pd-PHI	53	0.24	14
4	A-Pd-PHI	56	0.22	12

[a] BET specific surface area. [b] Specific pore volume. [c] Average pore diameter determined by the BJH method.

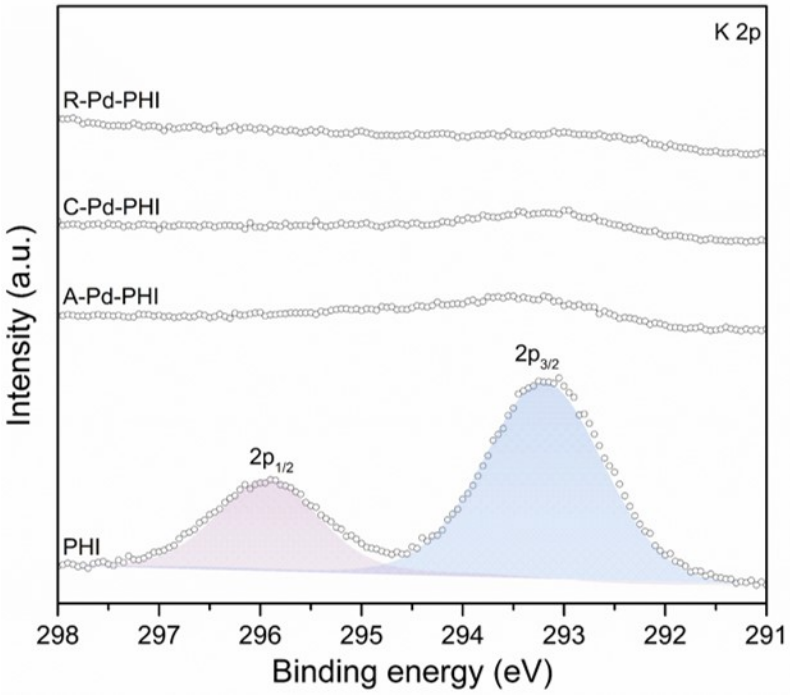

Figure S6. The K 2p X-Ray photoelectron spectra of the samples.

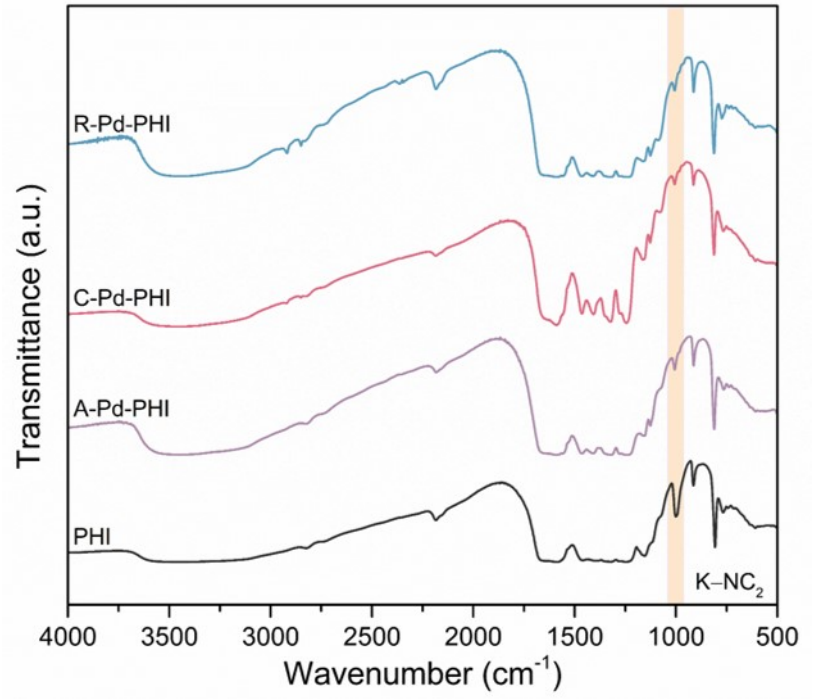

Figure S7. The FTIR spectra of the samples. Decrease of the peak intensity at ~1000 cm^{-1} is taken as the evidence of potassium removal from the PHI structure triggered by material exposure to acidic medium.

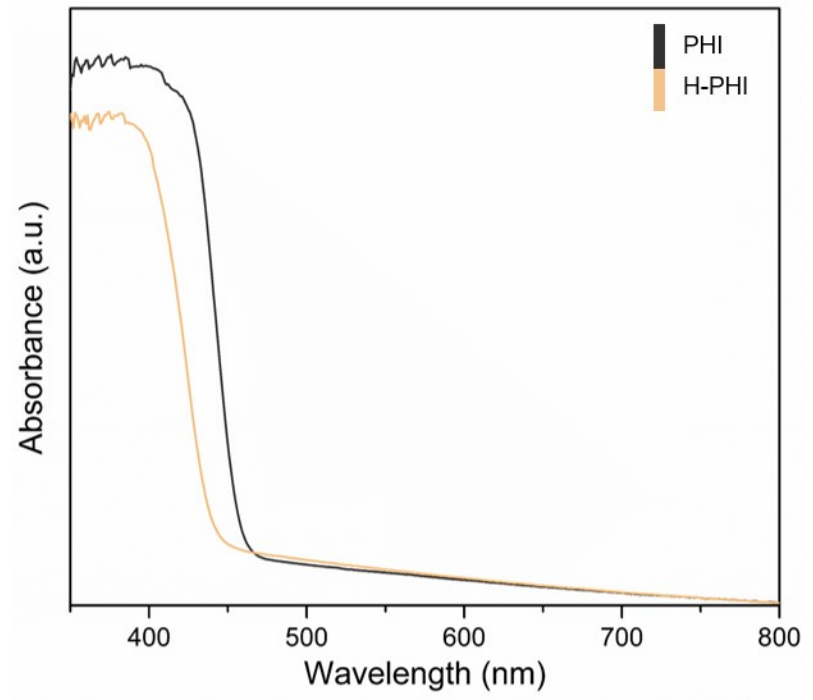

Figure S8. The UV–vis diffuse reflectance absorption spectra. (Note: The differences in the absorption spectra of PHI between Figure S7 and Figure 4a can be attributed to

differences in data acquisition instruments and batch-to-batch synthesis variations. However, these variations do not affect the validity of the conclusions drawn.)

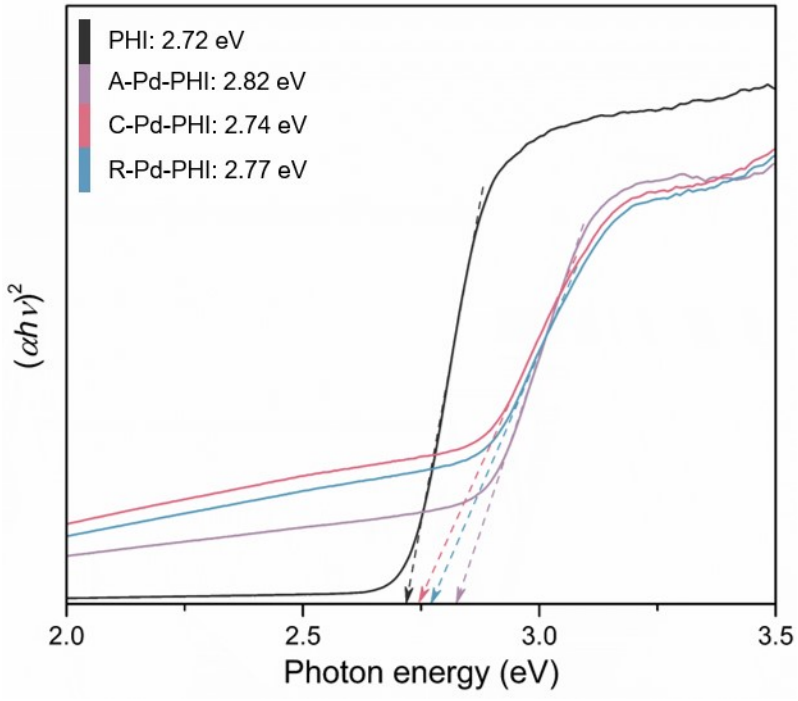

Figure S9. The band gaps determined from the Tauc plots.

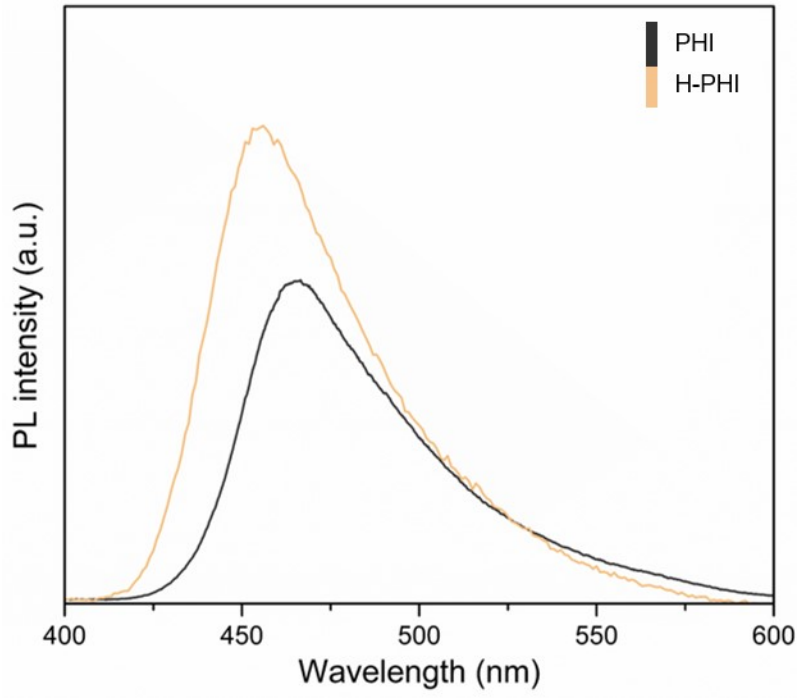

Figure S10. The PL spectra of the samples.

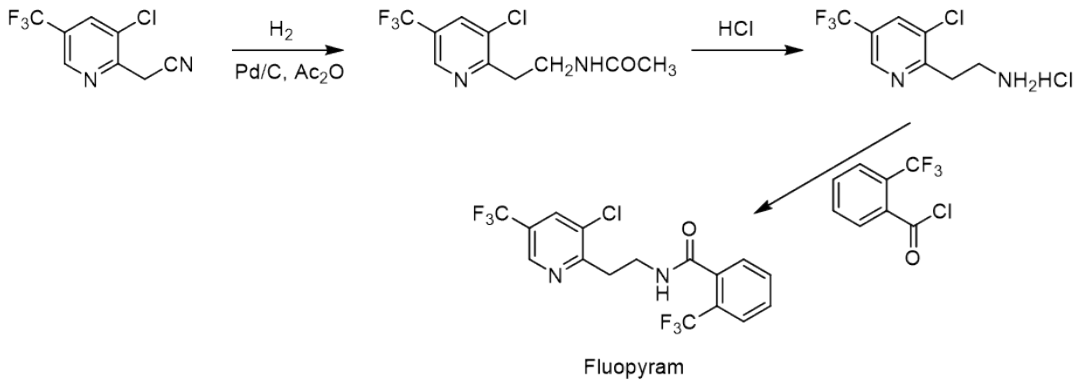

Figure S11. The synthetic route of fluopyram.

Table S3. Calculation of bond order in a series of nitriles.

Substrate	Laplacian bond order (C≡N)	Mayer bond order (C≡N)
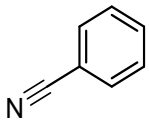	2.4976	3.1027
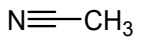	2.5307	3.1150
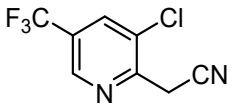	2.5392	3.1315

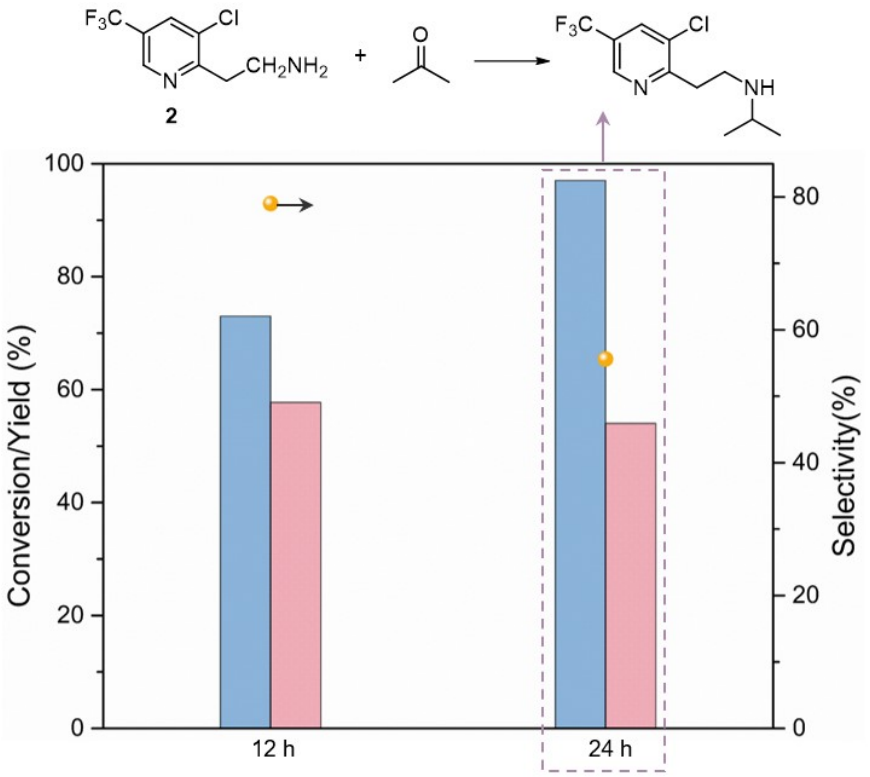

Figure S12. Time control experiments of the photocatalytic transfer hydrogenation.

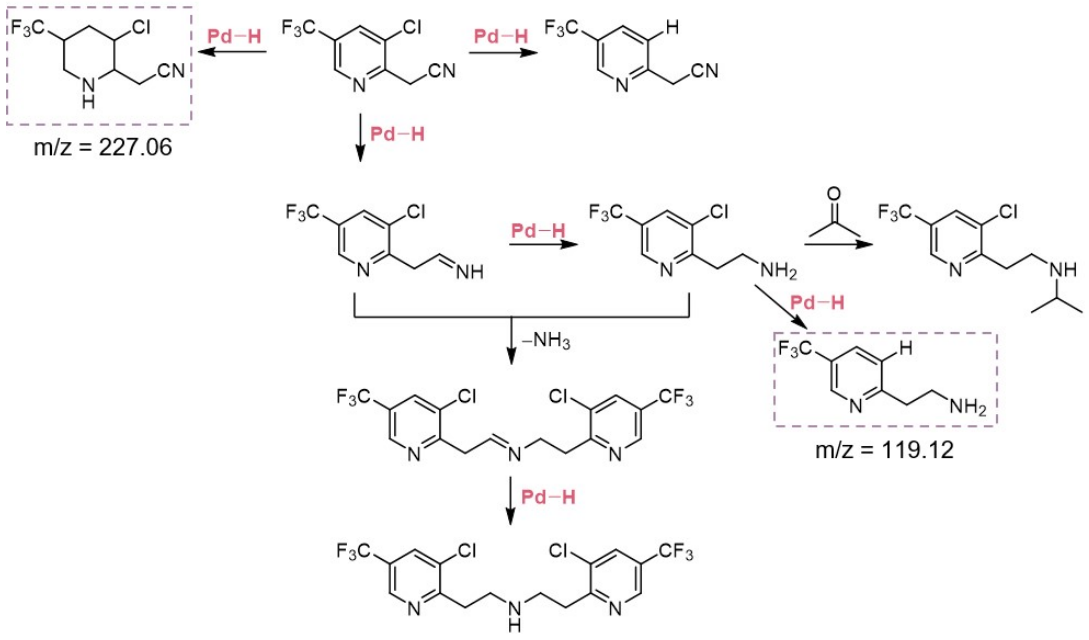

Figure S13. The possible hydrogenation process (The products in the parentheses can be observed in the mass spectrum of the reaction solution where A-Pd-PHI acts as the photocatalyst.).

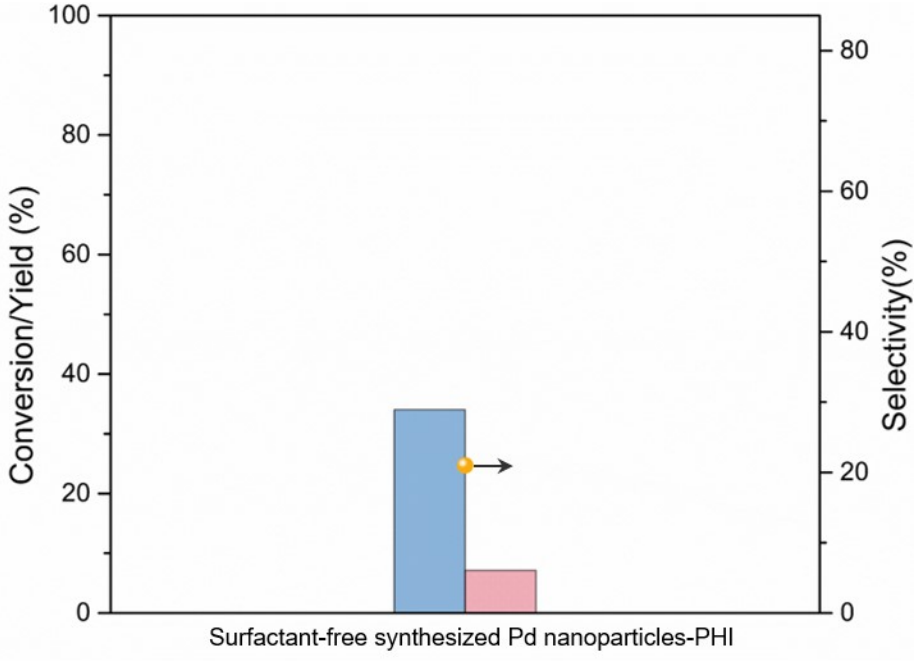

Figure S14. Photocatalytic transfer hydrogenation using surfactant-free synthesized Pd nanoparticles modified PHI as photocatalyst.

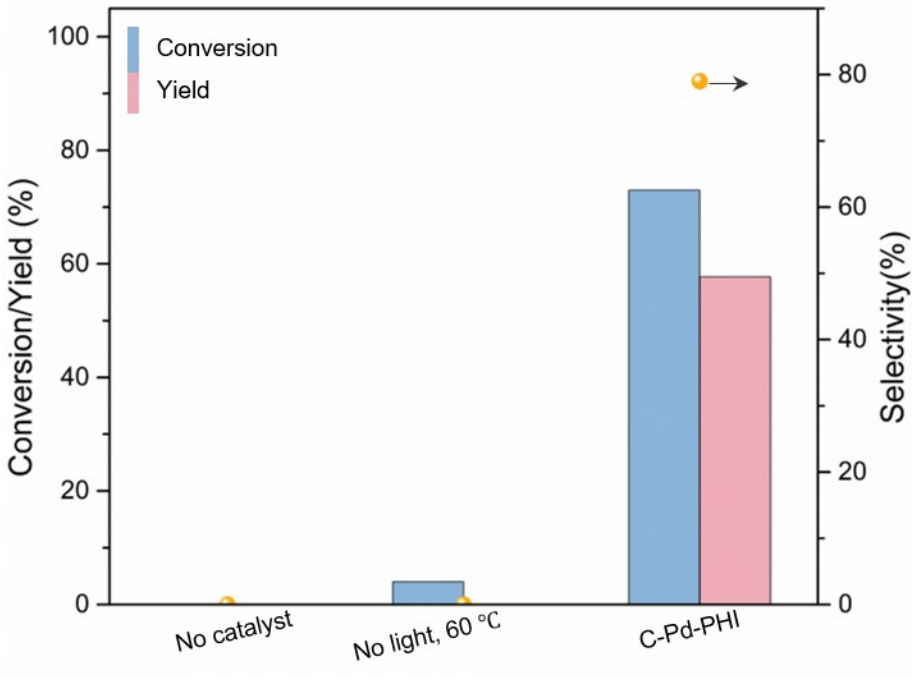

Figure S15. Photocatalytic transfer hydrogenation control experiments.

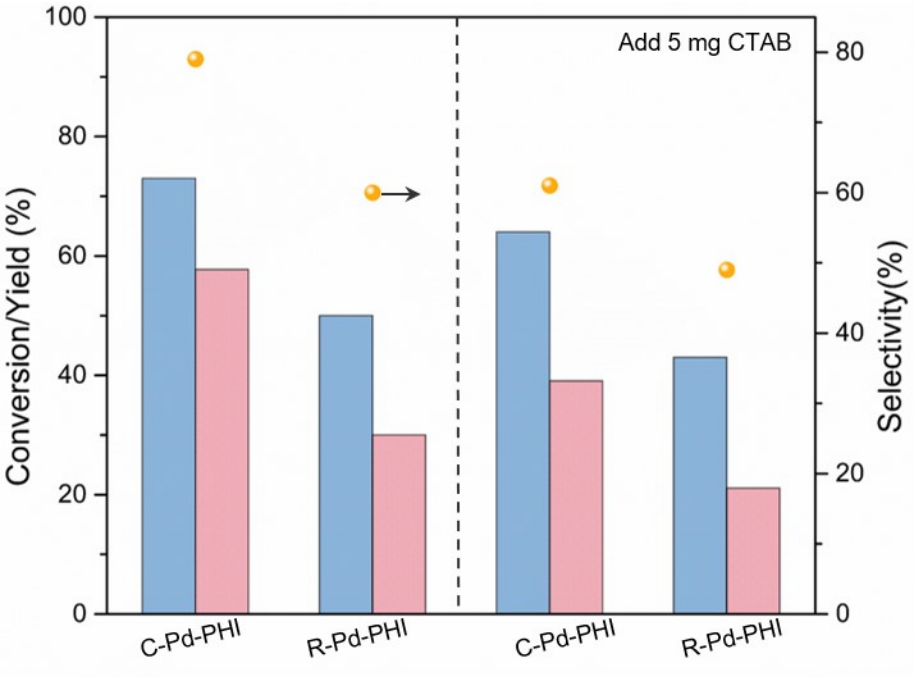

Figure S16. The influence of adding CTAB on the photocatalytic hydrogen transfer reaction.

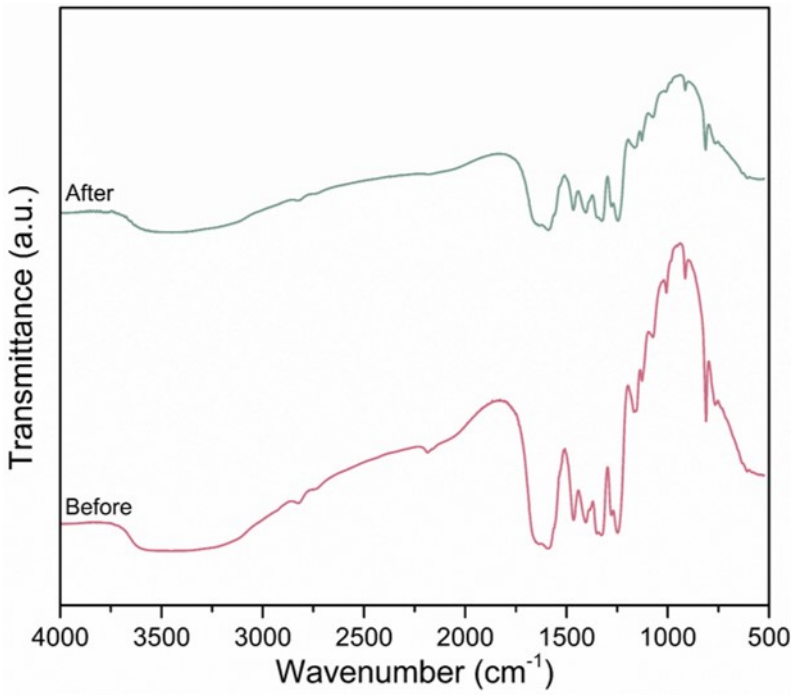

Figure S17. The FTIR spectra of C-Pd-PHI before and after 5th cycle of its use as the photocatalyst.

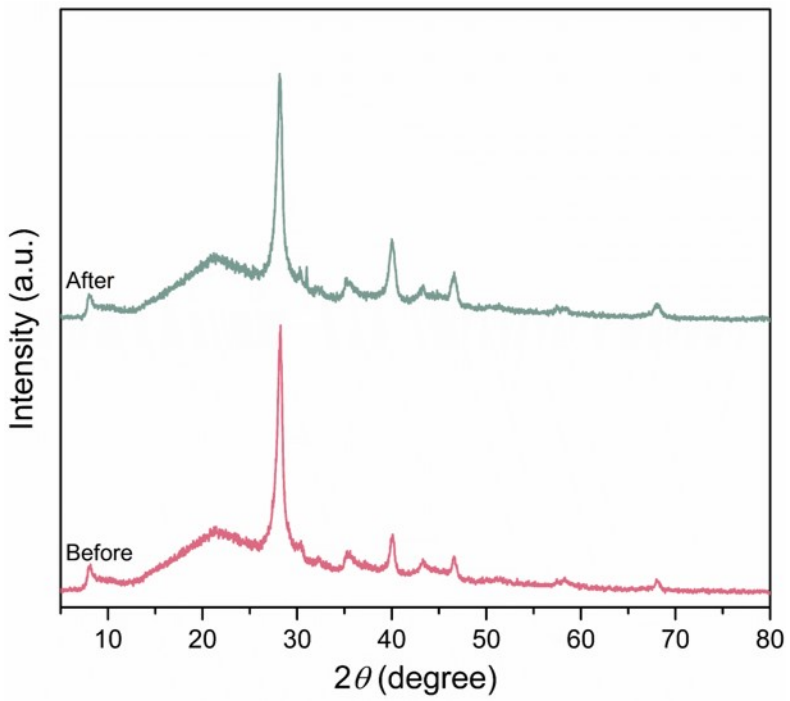

Figure S18. The powder XRD patterns of C-Pd-PHI before and after 5th cycle of its use as the photocatalyst.

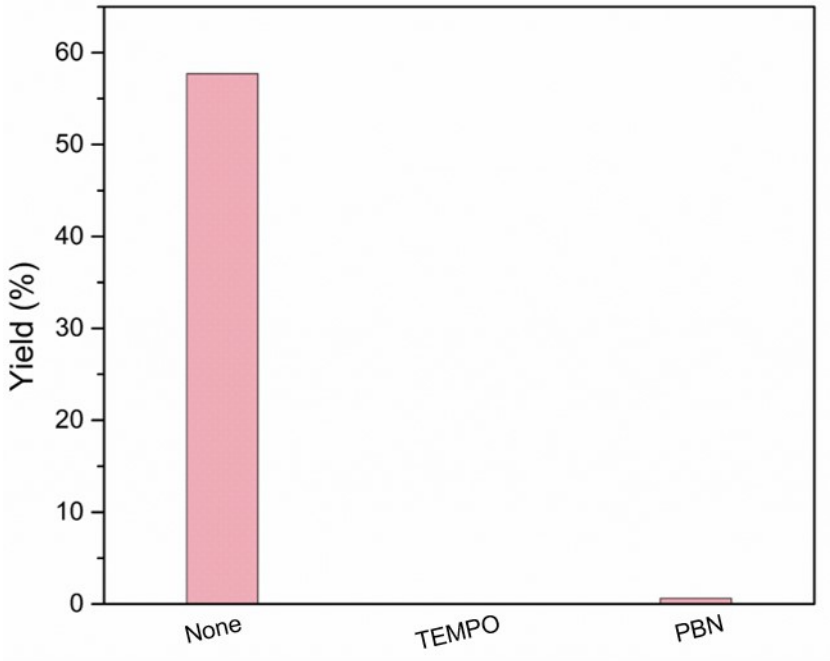

Figure S19. Trapping experiments using active species scavengers.

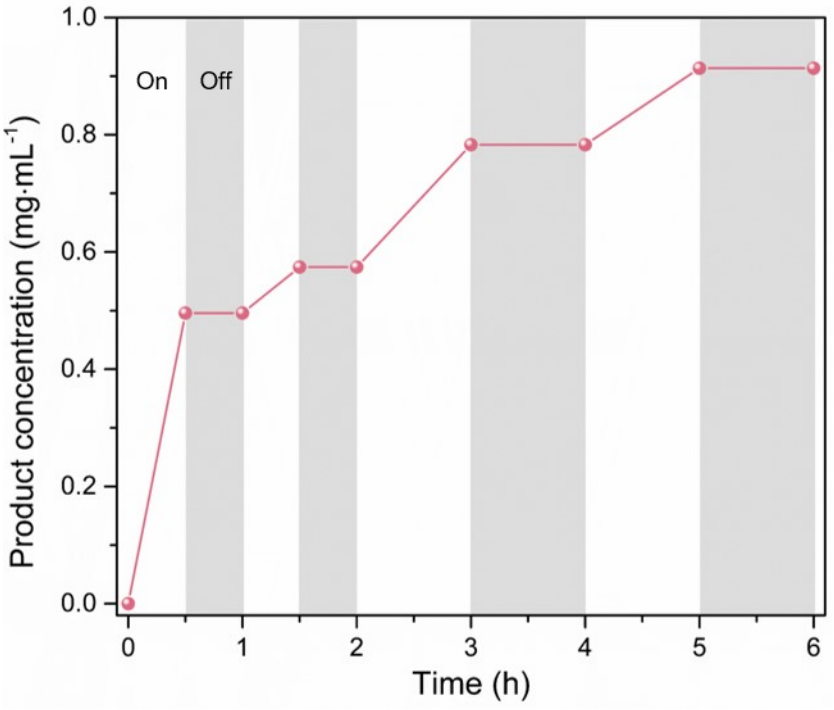

Figure S20. The concentration of **2** in the reaction mixture over the time with alternating light irradiation and dark intervals.

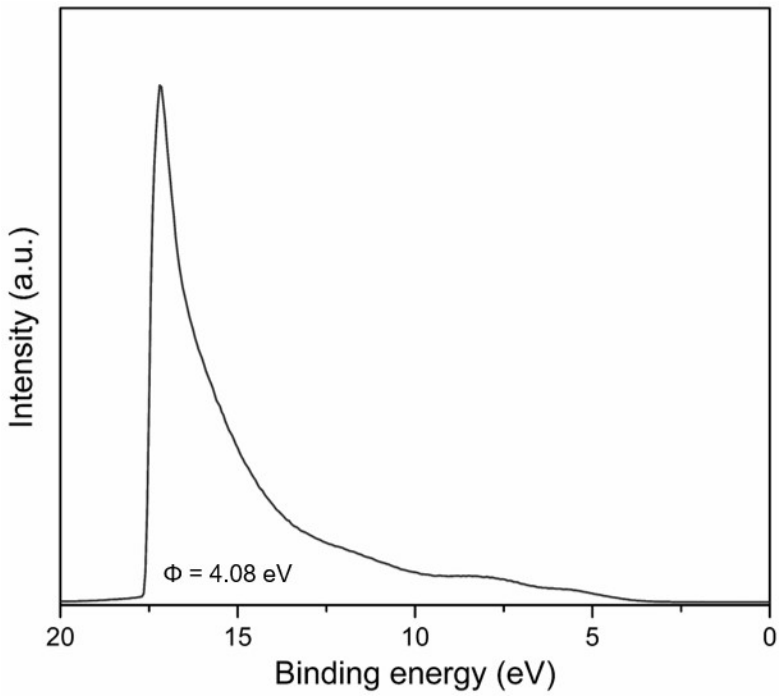

Figure S21. The UPS spectrogram of PHI.

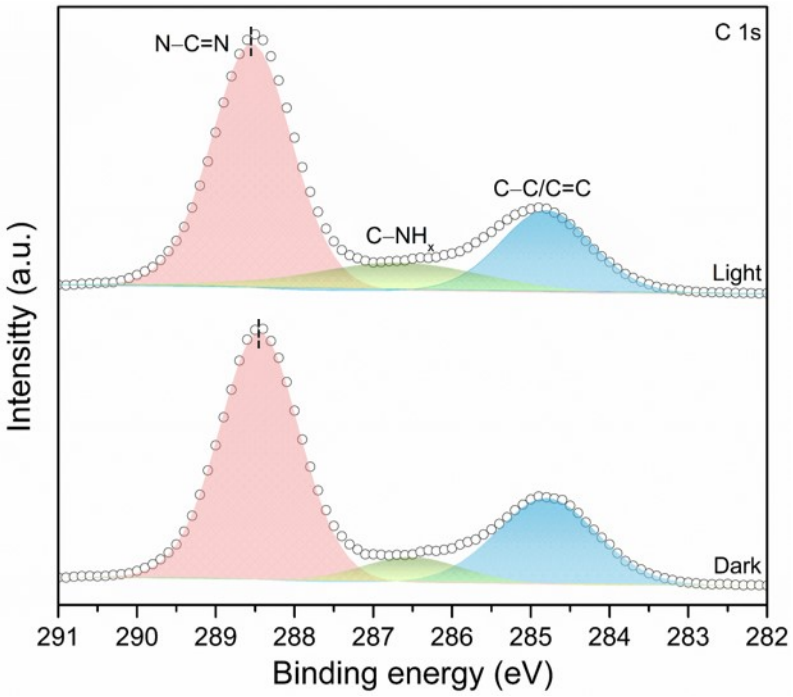

Figure S22. The XPS C 1s data of C-Pd-PHI (In situ XPS measurements were performed under 420 nm LED illumination).

S3 Reference

[S1] M. J. Frisch, G. W. Trucks, H. B. Schlegel, G. E. Scuseria, M. A. Robb, J. R. Cheeseman, G. Scalmani, V. Barone, G. A. Petersson, H. Nakatsuji, X. Li, M. Caricato, A. V. Marenich, J. Bloino, B. G. Janesko, R. Gomperts, B. Mennucci, H. P. Hratchian, J. V. Ortiz, A. F. Izmaylov, J. L. Sonnenberg, Williams, F. Ding, F. Lipparini, F. Egidi, J. Goings, B. Peng, A. Petrone, T. Henderson, D. Ranasinghe, V. G. Zakrzewski, J. Gao, N. Rega, G. Zheng, W. Liang, M. Hada, M. Ehara, K. Toyota, R. Fukuda, J. Hasegawa, M. Ishida, T. Nakajima, Y. Honda, O. Kitao, H. Nakai, T. Vreven, K. Throssell, J. A. Montgomery Jr., J. E. Peralta, F. Ogliaro, M. J. Bearpark, J. J. Heyd, E. N. Brothers, K. N. Kudin, V. N. Staroverov, T. A. Keith, R. Kobayashi, J. Normand, K. Raghavachari, A. P. Rendell, J. C. Burant, S. S. Iyengar, J. Tomasi, M. Cossi, J. M. Millam, M. Klene, C. Adamo, R. Cammi, J. W. Ochterski, R. L. Martin, K. Morokuma, O. Farkas, J. B. Foresman, D. J. Fox, Wallingford, CT **2016**.

[S2] T. Lu, F. Chen, *J. Comput. Chem.* **2012**, 33, 580.